TUNGSTEN ACCUMULATES IN THE INTERVERTEBRAL DISC AND VERTEBRAE STIMULATING DISC DEGENERATION AND UPREGULATING MARKERS OF INFLAMMATION AND PAIN

M.P. Grant[1], C.R. VanderSchee[2], H. Chou[1,3], A. Bolt[1], L.M. Epure[1] D. Kuter[2], J. Antoniou[1,4], S. Bohle[2], K.K. Mann[1,3] and F. Mwale[1,4,*]

[1] Lady Davis Institute for Medical Research, Jewish General Hospital, Cote Ste-Catherine Road, Montreal, QC, H3T 1E2, Canada
[2] Department of Chemistry, McGill University, 801 Sherbrooke St. W., Montreal, QC, H3A 0B8, Canada
[3] Department of Oncology, Division of Experimental Medicine, McGill University, Montréal, Québec, Canada
[4] Department of Orthopaedics, Division of Experimental Surgery, McGill University, Montréal, Québec, Canada

Abstract

Tungsten is incorporated in many industrial goods, military applications and medical devices due to its ability to impart flexibility, strength and conductance to materials. Emerging evidence has questioned the safety of tungsten exposure as studies have demonstrated it can promote tumour formation, induce pulmonary disease and alter immune function. Although tungsten is excreted from the body, it can accumulate in certain organs such as the brain, colon, liver, kidneys, spleen and bones, where most of the bioaccumulation occurs. Whether prolonged tungsten exposure leads to accumulation in other tissues is unknown. The present study demonstrated that mice exposed to 15 parts per million (ppm) sodium tungstate for 4 weeks in their drinking water showed comparable accumulation in both the bony vertebrae and intervertebral discs (IVDs). Lumbar IVD height was significantly reduced in tungsten-exposed mice and accompanied by decreased proteoglycan content and increased fibrosis. In addition to catabolic enzymes, tungsten also increased the expression of the inflammatory cytokines IL-1β and tumour necrosis factor (TNF)-α as well as the neurotrophic factors nerve growth factor (NGF) and brain-derived nerve factor (BDNF) in IVD cells. Tungsten significantly increased the presence of nociceptive neurons at the endplates of IVDs as observed by the expression of calcitonin gene-related peptide (CGRP) and anti-protein gene product 9.5 (PGP9.5) in endplate vessels. The present study provided evidence that tungsten may enhance disc degeneration and fibrosis as well as increase the expression of markers for pain. Therefore, tungsten toxicity may play a role in disc degeneration disease.

Keywords: Low-back pain, tungsten, intervertebral disc, degeneration, medical devices, pain.

***Address for correspondence**: Fackson Mwale, PhD, FIOR, SMBD-Jewish General Hospital, Lady Davis Institute for Medical Research, 3755 Cote Ste-Catherine Road, Room F-602, Montreal, QC, CAN, H3T 1E2. Telephone number: +1 5143408222 Email: fmwale@jgh.mcgill.ca

List of Abbreviations

Acan	aggrecan
ADAMTS	a disintegrin and metalloproteinase with thrombospondin motifs
AF	annulus fibrosus
BDNF	brain-derived nerve factor
BEI	backscattered electron imaging
BSA	bovine serum albumin
CGRP	calcitonin gene-related peptide
Col1a1	type I collagen
Col2a1	type II collagen
DHI	disc height index
DMMB	dimethyl methylene blue
GAG	glycosaminoglycan
HYP	hydroxyproline
ICP-MS	inductively coupled plasma mass spectrometry
IL	interleukin
IVD	intervertebral disc

LA-ICP-MS	laser ablation ICP-MS
MMA	methyl methacrylate
MMPs	matrix metalloproteinases
NGF	nerve growth factor
NP	nucleus pulposus
PBS	phosphate-buffered saline
PGP9.5	anti-protein gene product 9.5
ppb	parts per billion
ppm	parts per million
ppt	parts per trillion
ROS	reactive oxygen species
SD	standard deviation
SEM	standard error of the mean
SR-μXRF	synchrotron radiation micro X-ray fluorescence
SRX	sub-micron resolution X-ray spectroscopy
TNF	tumour necrosis factor
VEGF	vascular endothelial growth factor

Introduction

The spine is composed of vertebral segment units consisting of a bony vertebrae and the IVD. IVDs link two adjacent vertebrae and are composed of the collagen-rich AF, the central gel-like proteoglycan-rich NP and two endplates of hyaline cartilage that sandwich the AF and NP (Oegema, 1993; Vo *et al.*, 2016). The compressive ability of the NP is achieved by the attraction of water molecules from the GAG chains present on individual aggrecan monomers (the principal proteoglycan in the disc) (Oegema, 1993; Watanabe *et al.*, 1998).

IVD degeneration is considered one of the underlying factors of low-back pain and disability worldwide (Hoy *et al.*, 2014). In the early stages of IVD degeneration, there is an imbalance in disc matrix homeostasis typified by an increase in the expression and activity of catabolic enzymes such as ADAMTS-4 and -5 and MMP-3 and -13, presumably due to elevations in the inflammatory cytokines IL-1β and TNF-α and free calcium, respectively (Grant *et al.*, 2016; Sampara *et al.*, 2018). This process results in the degradation of aggrecan and, as the NP losses water, it becomes more fibrotic, eventually leading to the formation of clefts that can also affect the integrity of the AF. Sequelae of enhanced inflammatory cytokines eventually lead to increases in the expression of the neurotrophic factors NGF and BDNF from disc cells, resulting in hyperinnervation of the IVD (Johnson *et al.*, 2015; Noorwali *et al.*, 2018).

Tungsten (W, atomic number 74) is a naturally occurring transition element, belonging in group 6 of the periodic table. It is the only third row transition metal with a known natural biochemistry. As a result of its unique material characteristics, such as the highest melting point of any metal, high density, high tensile strength, flexibility and good conductive properties, tungsten is an extremely useful element having broad medical, industrial, civil and military applications (Bolt and Mann, 2016; Zoroddu *et al.*, 2018). These range from daily household goods, such as light bulb filaments and golf clubs, to electronics, hard metal tools, welding electrodes, turbine blades, munitions, X-ray equipment and implanted medical devices. Given its widespread use, there have been increasing reports of tungsten detection and movement in potable water and ground sources, as materials that are left in the environment can become bioaccessible as tungstate and lead to population exposure (Keith *et al.*, 2007a; Keith *et al.*, 2007b; Lemus and Venezia, 2015).

Since tungsten is in many projectile munitions, veterans are particularly at risk of tungsten exposure through inhalation of particles and embedment of shrapnel from detonated ammunition and improvised explosive devices. Tungsten concentrations in the urine of several veterans were significantly higher (11.6 %) than the upper reference limit established in the National Health and Nutrition Examination Survey NHANES Database (0.003-2.70 μg/g creatinine) (Gaitens *et al.*, 2017). In addition to occupational exposure, increased concentration of tungsten has been observed in blood and urine from patients with tungsten-based medical therapies (Domingo, 2002; Lalak and Moussa, 2002; Tajima, 2001; Tajima, 2003). For instance, tungsten coils used in peripheral vascular embolisation procedures have been reported to corrode and degrade over time increasing urinary tungsten concentration in patients with these implants (Bachthaler *et al.*, 2004; Barrett *et al.*, 2000; Bolt and Mann, 2016; Lalak and Moussa, 2002). In a cohort study on breast cancer, patients who were implanted with a tungsten-based shield during intra-operative radiotherapy treatment presented with elevated serum tungsten levels even after the shield was removed (Bolt *et al.*, 2015).

Although tungsten is rapidly excreted from the body through the kidneys, it bioaccumulates in certain organs namely bones, spleen, colon, kidneys, liver and brain (Guandalini *et al.*, 2011). Bone tissue represents the primary site of tungsten accumulation and storage, with a slow rate of removal (Guandalini *et al.*, 2011; Kelly *et al.*, 2013; Leggett, 1997; VanderSchee *et al.*, 2018). In a recent report, tungsten was shown to enhance the adipogenesis of bone marrow-derived mesenchymal stem cells while inhibiting osteogenesis (Bolt *et al.*, 2016). In a relationship study between environmental exposures and the onset of the ankylosing spondylitis (a common form of inflammatory arthritis of the spine affecting spine mobility), tungsten urinary levels were found to be positively correlated (Shiue, 2015). However, to date, there are no studies that have investigated the distribution of tungsten in vertebrae and IVDs and its potential contribution to the development of low-back pain.

The present study describes for the first time ~~that~~ that tungsten can accumulate *in vivo* and alter the biochemistry of the disc following oral exposure to sodium tungstate.

Materials and Methods

Materials

Sodium tungstate (72069) was purchased from Sigma-Aldrich. Anti-aggrecan (ab36861), anti-collagen type I (ab34710), anti-collagen type II (ab34712), anti-ADAMTS-4 (ab185722), anti-IL-1β (ab2105), anti-NGF (ab52918), anti-CGRP (ab81887) and anti-PGP9.5 (ab8189) antibodies were purchased from Abcam (Cambridge, UK). Anti-VEGF antibody (sc-7269) was purchased from Santa Cruz Biotechnology.

In vivo exposure

All animal experiments were approved by the McGill University Animal Care Committee (Montreal, Quebec, Canada). Wild-type C57BL/6 mice (male, 5 weeks old) were purchased from Charles Rivers Laboratories Inc. (Montreal, Quebec, Canada) and housed at the Lady Davis Institute Animal Care Facility. Mice were given food and water a*d libitum*. For *in vivo* tungsten exposures, mice were divided into 2 groups: control tap water (n = 15) or 15 ppm (mg/L) tungsten (sodium tungstate) (n = 18). Sodium tungstate dehydrate ($Na_2WO_4 \cdot 2H_2O$; Sigma-Aldrich) was dissolved in tap water and replaced every 2 or 3 d to limit conversion to polytungstates (Kelly *et al.*, 2013). The concentration of tungsten used represented elemental tungsten as opposed to the dihydrate compound (1.795 g Na_2WO_4–$2H_2O$ for 1 g tungsten). After 1 week of acclimatisation, mice were exposed to tap water or tungsten in drinking water for 4 weeks (Bolt *et al.*, 2016; 2015). Effects on body weight and urine analysis have been previously published (Bolt *et al.*, 2016; 2015). To determine the diffusion of tungsten from the IVD, tungsten-exposed animals were put on a washout period for 12 weeks with regular tap water *ad libitum* (n = 3). For SR-μXRF and LA-ICP-MS, mice were exposed for 4 weeks to 1,000 ppm tungsten. Although 1,000 mg/L is higher than tungsten concentrations in environmental water measurements (VanderSchee *et al.*, 2018), these concentrations were chosen to provide significant accumulation in disc and bone for visualisation with SR-μXRF and LA-ICP-MS techniques. After the 4-week exposure, mice were euthanised by CO_2 asphyxiation followed by terminal cardiac puncture.

Tungsten analysis

Tungsten concentrations in the IVDs and vertebrae were quantified by ICP-MS, as previously described (Bolt *et al.*, 2016; Kelly *et al.*, 2013; VanderSchee *et al.*, 2018). Data were reported as mean tungsten concentration (ppb) per weight of vertebral bone or IVD. The elemental limit of detection was set to 100 ppb.

LA-ICP-MS sample preparation

Vertebral samples were dissected and placed for 1 week in a solution of 4 % paraformaldehyde for fixation. Then, specimens were washed 3 times with a solution of 1 % PBS at pH 7.4 and stored in the same solution. For mounting, samples were dehydrated using a series of ethanol incubations followed by xylene and MMA before finally being set.

Mounted samples were cut using a diamond saw before being polished using 600 grit silicon carbide paper and 6 and 1 μm diamond suspension. This treatment resulted in losing the lumbar disc but provided high integrity vertebra samples.

BEI sample preparation and measurement

Polished surfaces from LA-ICP-MS preparation were carbon coated for BEI. BEI measurement was performed on a FEI Inspect F50 FE-SEM with EDAX Octane Super 60 mm^2 SDD and TEAM EDS Analysis System. Thin sections of the samples were prepared by cutting using a diamond saw and further grinding down the back of the samples using 120 grit silicon carbide paper to approximately 100-250 μm, leaving the surface untouched for LA-ICP-MS measurements.

LA-ICP-MS measurement

LA-ICP-MS measurements were performed at the Dartmouth Trace Element Analysis Lab and were carried out using a NWR213 laser (Elemental Scientific Lasers, Bozeman, MT, USA). Elemental detection was performed using an Agilent 7900 ICP-MS set to monitor S, Ca, Fe, Zn, W, Zn (at m/z 34, 43, 56, 66 and 182, respectively) in hydrogen mode. Sampling parameters included laser settings of 15 μm spot diameter, laser scan speed of 30 μm/s firing at 20 Hz and laser power set at 50 % equating to a fluence of 12.9 J/cm^2. Data were collected as time resolved intensity of S, Ca, Fe, Zn, W, Zn with a sampling period of 0.5 s so that each data pass of the ICP-MS corresponded to 15 μm on the sample. A 15 μm spot size was chosen for elemental mapping. LA-ICP-MS data were plotted using MatLab R2017b (Web ref. 1). A histogram analysis was performed on the intensity data to determine upper and lower limits of LA-ICP-MS plots. These values were selected such as to exclude the bottom and top 0.5 % of the outlying data.

SR-μXRF measurement

Samples for SR-μXRF were prepared using fresh vertebra sections, placed between strips of Kapton tape and stored frozen until use. SR-μXRF measurements were performed at the National Synchrotron Light Source II (NSLS-II) at the 5ID beamline. The SRX beamline, located at 5-ID of the NSLS-II, is fed by an in-vacuum undulator. The high-brightness white beam is incident upon a harmonic rejection mirror and then into a fixed-exit Si(111) double-crystal monochromator, both of which deflect the beam horizontally. The monochromatic X-ray beam passes through a secondary source plane. In the "high flux" mode, the harmonic rejection mirror is bent to produce a ~ 70 μm image of the primary source in this plane; in the "high energy resolution" mode, the mirror is flattened and an aperture forms the secondary source in the horizontal direction.

The current work was performed in the "high-flux" geometry, which serves as the effective source for the final focusing optics, a Kirkpatrick-Baez mirror pair. These fixed-figure mirrors are designed to produce a slightly sub-μm X-ray spot on the sample. To collect an X-ray fluorescence map, the sample was scanned through this beam on a crossed pair of stages with a continuous travel range of 50 mm (height) × 40 mm (width) measured with a 5 nm encoder resolution. Spot size of the elemental map was chosen to be 20 μm. XRF data obtained from the NSLS-II were deconvoluted using the PyXRF software package (Web ref. 2). Data were normalised by incident beam count values and graphed in MatLab R2017b. A histogram analysis was performed on the intensity data to determine upper and lower limits of SR-μXRF plots. These values were selected such as to exclude the bottom and top 0.5 % of the outlying data.

Cell isolation, RNA extraction and quantitative real-time PCR

Bovine NP and AF cells were isolated from 4 different bovine caudal tails from 22-24-month-old steers. NP or AF tissue was excised from the disc using a scalpel. Tissue was chopped in small pieces and placed in a 50 mL conical tube. Tissue was washed twice for 5 min in 2× volume of PBS containing antibiotics (1 % penicillin/streptomycin and 1 % Fungizone). Then, NP and AF tissue was incubated for 1 h in PrimeGrowth® Disc Cell Medium (319-515-CL, Wisent Bioproducts, Montreal, Canada) containing 0.125 % pronase [1.5× weight (g) in volume (mL)]. Tissue was washed twice for 5 min in PrimeGrowth® Disc Cell Medium. NP and AF tissues were digested overnight at 37 °C while rocking in 0.2 mg/mL collagenase I or 0.2 mg/mL collagenase II (1.5× weight in volume), respectively, in PrimeGrowth® Disc Cell Medium containing antibiotics. Then, cellular suspension was filtered using a 100 μm cell strainer. Cellular suspension was centrifuged for 10 min at 760 ×*g* and pellet was washed twice using PrimeGrowth® Disc Cell Medium. Cells were counted and cultured in flasks using PrimeGrowth® Disc Cell Medium supplemented with 10 % FBS and antibiotics. Cells were passaged up to passage 3 before discarding. Medium was replaced every 3 d. For gene expression experiments, cells were cultured as micro-pellets at a density of 2.5×10^5 cells/pellet prior to treatment. Pellets were treated for 6 d with tungsten (15 ppm) or PBS (vehicle) as a control. Total RNA was extracted using a total RNA mini-kit (Geneaid Biotech Ltd., New Taipei City, Taiwan) following manufacturer instructions. Complimentary DNA was synthesised using a superscript Vilo cDNA synthesis kit (Thermo

Table 1. Primers for gene expression. F: forward. R: reverse.

Gene	Primer sequence
Gapdh	F: 5′-GCTCTCCAGAACATCATCCCTGCC-3′ R: 5′-CGTTGTCATACCAGGAAATGAGCTT-3′
Acan	F: 5′-TGAGTCCTCAAGCCTCCTGT-3′ R: 5′-CCTCTGTCTCCTTGCAGGTC-3′
Col1a1	F: 5′-GAGAGCATGACCGATGGATT-3′ R: 5′-CCTTCTTGAGGTTGCCAGTC-3′
Col2a1	F: 5′-ATGACAATCTGGCTCCCAAC-3′ R: 5′-CTTCAGGGCAGTGTACGTGA3′
Adamts4	F: 5′-TCCTGCAACACTGAGGACT-3′ R: 5′-GGTGAGTTTGCACTGGTCC-3′
Adamts5	F: 5′-ACAAGGACAAGAGCCTGGAA-3′ R: 5′-ATCGTCTTCAATCACAGCACA-3′
Mmp1	F: 5′-AAAGGGAATAAGTACTGGG-3′ R: 5′-GTTTTTCGAGTGTTTACCTCAG-3′
Mmp3	F: 5′-GGCAGTTTGCTCAGCCTATC-3′ R: 5′-GAGTGTCGGAGTCCAGCTT-3′
Mmp13	F: 5′-TAAGGAGCATGGCGACTTC-3′ R: 5′-GGTCCTTGGAGTGGTCAAG-3′
Il1	F: 5′-ACCTATCTTCTTCGACACATG-3′ R: 5′-ACCACTTGTTGCTCCATATCC-3′
Tnfa	F: 5′-ACCACGCTCTTCTGCCTGCTG-3′ R: 5′-TACAACATGGGCTACAGGCTT-3′
Ngf	F: 5′-TCAGCATTCCCTTGACACTG-3′ R: 5′-TGCTCCTGTGAGTCCTGTTG-3′
Bdnf	F: 5′-GGCTGACACTTTCGAACACA-3′ R: 5′-AGAAGAGGAGGCTCCAAAGG-3′

Fisher Scientific). Quantitative real-time PCR of genes listed in Table 1 was performed using the Applied Biosystems™ 7500 Real-Time PCR Systems with SYBR™ Green Master Mix (Thermo Fisher Scientific) and specific primers. Relative mRNA expression level was normalised to controls as previously described (Antoniou *et al.*, 2012).

GAG analysis

Sulphated GAGs were quantified in tissue extracts by a modified DMMB dye-binding assay as previously described (Barbosa *et al.*, 2003; Mort and Roughley, 2007). Samples were diluted to fall within the middle of the linear range of the standard curve. Extraction buffer of an equal volume as the tissue extracts was added to the standard curve to compensate for possible interference.

HYP content

HYP content was measured as previously described (Yee *et al.*, 2016). Proteinase K tissue digests were used for analysis of HYP as a measure of total collagen content. For analysis, digests were hydrolysed in 6 mol/L HCl to release free HYP, which was then quantitated using dimethylaminobenzaldehyde (Burleigh *et al.*, 1974). Total collagen content was estimated assuming that HYP content is equivalent to 10 % of the weight of each collagen α chain (Nimni, 1983).

Histology and immunohistochemistry

The lumbar vertebral spines of the tungsten-exposed and control animals were dissected and fixed in Accustain (Millipore) followed by decalcification in Osteosoft (Millipore). The lower vertebrae (L1-L5) from 4 individually treated mice were paraffin-wax embedded sagittally and used for histological assessment and immunohistochemistry. Sections were prepared mid-sagittally (approximately 3 mm into the tissue depending on the thickness of the spine) and blocked using VECTASTAIN® ABC kit (Vector Laboratories) followed by incubation overnight at 4 °C with the indicated primary antibodies [1 : 500] diluted in Tris-buffered saline (Millipore) buffer containing 1 % BSA. Secondary antibody and further processing of slides was performed using VECTASTAIN® ABC kit following manufacturer's guidelines. Substrate and development were processed using DAB Substrate Kit (Vector Laboratories). Sections were counterstained with haematoxylin, dehydrated by a graded series of percent ethanol concentrations and HISTO-CLEAR (Thermo Fisher Scientific) and mounted using Permount™ Mounting Medium (Thermo Fisher Scientific). Positive cells were validated based on immunohistochemistry reaction. Antibody control demonstrated no discernible staining on the discs from control or tungsten-treated animals (data not shown).

Statistical analysis

Data were analysed by two-way ANOVA followed by *post-hoc* Sidak multiple comparison's test or by a Mann-Whitney non-parametric test, where indicated. A $p < 0.05$ was considered statistically significant.

Results

Due to the accumulation of tungsten in long bones (Bolt *et al.*, 2016), the present study examined whether tungsten also accumulated in the vertebrae and associated IVDs and whether this altered spine parameters. After exposing mice to 15 ppm tungsten through sodium tungstate (Na_2WO_4) in drinking water over the course of 4 weeks, vertebrae and IVDs showed increased tungsten levels when compared to control (Fig. 1**a**). When compared to vertebrae or IVD baseline concentrations, which were approximatively 100 ppb, in animals on tungsten diet, vertebral concentrations increased to approximatively 3,000 ppb ($p < 0.0001$). These findings were consistent in either the vertebral bone or disc tissue (Fig. 1**a**).

BEI showed dense, calcium-containing cortical and cancellous bone but not lighter organic material, providing a reference image of bone morphology (Fig. 1**b**). Localised accumulation of tungsten in vertebrae was investigated by LA-ICP-MS in the discs from the spines of 3 animals. Tungsten accumulation was observed throughout the vertebrae, including localisation at the endplate (Fig. 1**c**). As the method for preparing samples for LA-ICP-MS resulted in IVD loss, a scanning confocal SR-μXRF was used to examine the distribution of tungsten in IVDs [since this non-destructive technique is a powerful analytical tool for qualitative analysis of the chemical elements present in the sample (Szalóki *et al.*, 2004; VanderSchee *et al.*, 2018)]. Recently, SR-μXRF has been used to determine the spatial distribution and speciation of tungsten in bone (VanderSchee *et al.*, 2018). The results of the present study revealed that tungsten was present in the IVD. The intensity map showed strikingly increased fluorescence intensities in the AF (Fig. 1**d**, central panel, W). Disc from control mice demonstrated little to no fluorescent tungsten signatures (Fig. 1**d**, left panel, CTL). To determine if tungsten remained in the IVD or was readily diffusible, mice that were on a tungsten diet for 4 weeks were subjected to a washout period of 12 weeks by allowing them access to regular tap water. Surprisingly, intense fluorescent tungsten signatures were still visible in the IVD (Fig. 1**d**, right panel).

Tungsten accumulation at high concentrations in IVDs and vertebrae raised concerns about its effects on the spine. Following exposure of mice to tungsten, the disc height index of lumbar IVDs were significantly diminished ($p = 0.0286$) compared with control (Fig. 2).

GAG concentration was measured in the discs because of the major role proteoglycans play in the functional ability of IVDs to swell and resist compressive forces (Sampara *et al.*, 2018). There was a significant decrease in GAG content ($p = 0.0022$) in discs from the tungsten group when compared with

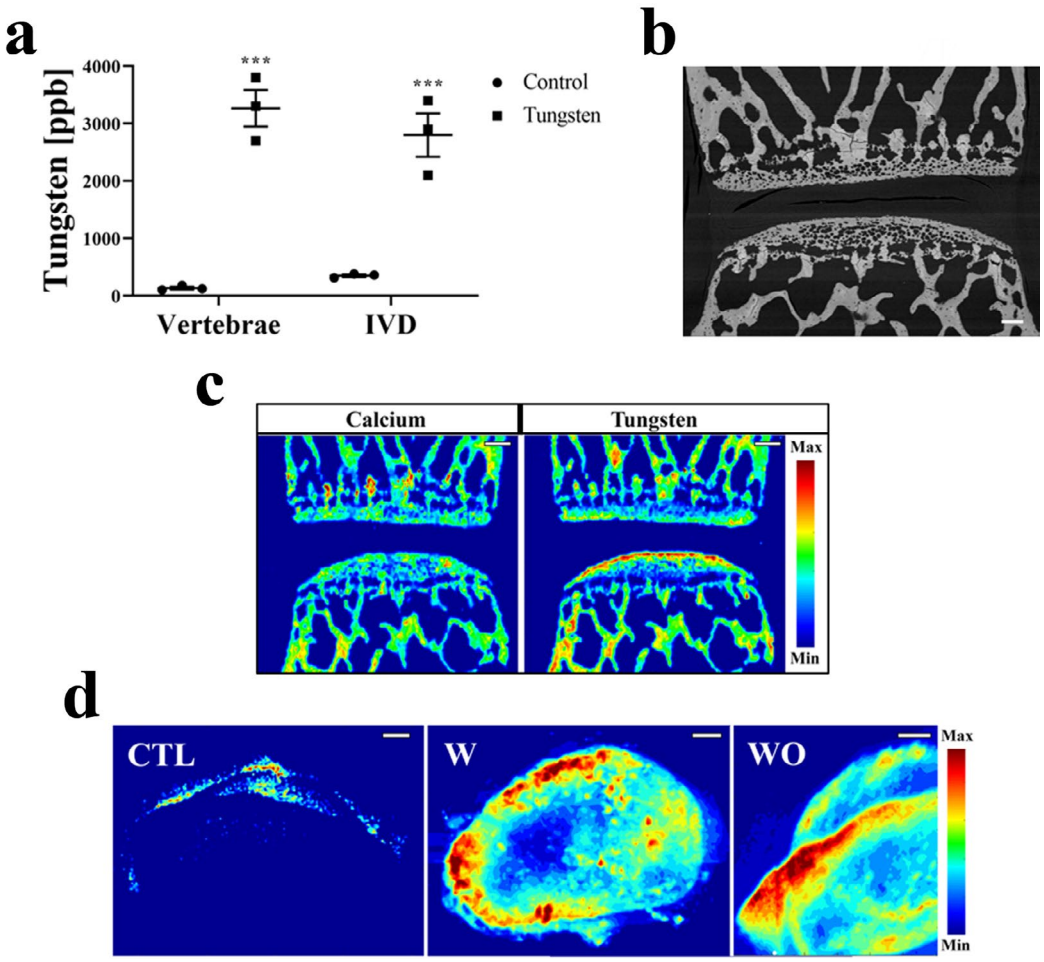

Fig. 1. Tungsten accumulation in murine spines. (**a**) ICP-MS data on tungsten content in lumbar vertebrae and IVDs following exposure to 15 ppm tungsten in the drinking water for 4 weeks. Control animals were given regular tap water. Means ± SDs; $n = 3$. Two-way ANOVA, *post-hoc* Bonferroni, *** $p < 0.001$. (**b**) A representative BEI of a murine lumbar spinal segment following 4 week exposure to 1,000 ppm tungsten. (**c**) LA-ICP-MS map of calcium and tungsten from identical spinal segments as displayed in **b**. (**d**) SR-μXRF map of tungsten in an isolated lumbar disc from control (left panel, CTL) and 1,000 ppm tungsten-exposed mice (central panel, W). SR-μXRF map of a lumbar disc from a mouse exposed to 1,000 ppm tungsten for 4 weeks followed by a washout for 12 weeks (mouse on regular tap water; right panel, WO). Scale bar: 200 μm.

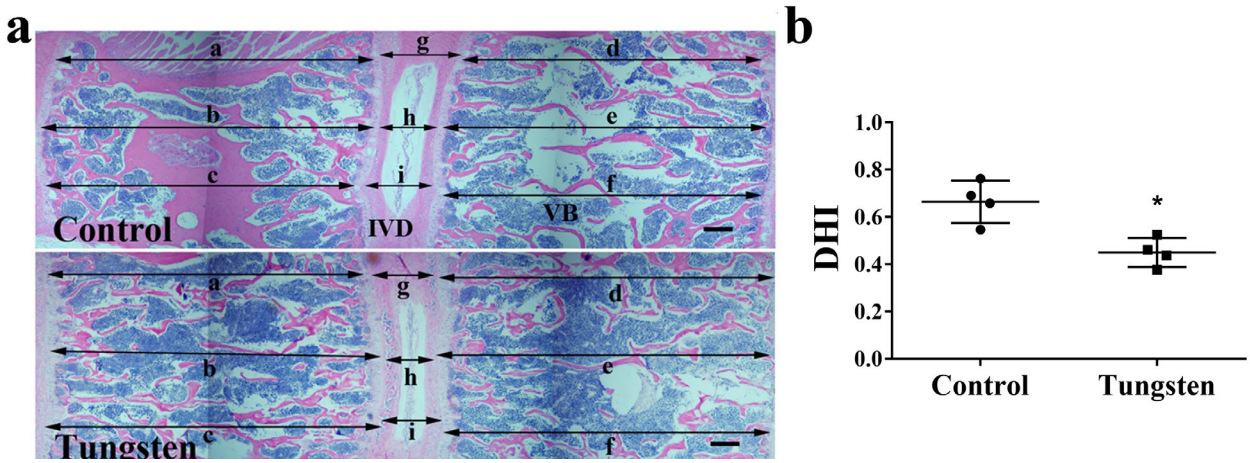

Fig. 2. Effect of disc height following tungsten exposure. (**a**) Representative images of vertebral bodies (VB) and IVD from the lumbar region of control and tungsten-exposed mice sections stained with haematoxylin and eosin. Scale bar: 100 μm. (**b**) DHI was calculated by measuring the lengths of the VB and IVD as follows: DHI = [2 × (g + h + i)/(a + b + c + d + e + f)]. Dots represent average result of lumbar discs (L1-5) of individual animals. Lines represent means ± SEMs; Mann-Whitney test, * $p < 0.05$; $n = 4$ animals.

control after 12 weeks, indicative of proteoglycan (aggrecan) loss (Fig. 3**a**). HYP, as an indicator of disc collagen content, was measured due to the intimate role that collagen plays in the mechanical strength of IVDs and its resistance to swelling. The discs responded to tungsten exposure by significantly increasing their collagen content as compared with control ($p = 0.0022$) (Fig. 3**b**).

An extracellular matrix with a high proteoglycan to collagen ratio can be used as a means to identify an NP-like phenotype *in vivo* as an indicator of disc degeneration (Mwale *et al.*, 2004). In control discs, the GAG to collagen ratio in the disc was on average 3.7 : 1 (Fig. 3**c**). Following tungsten exposure, the GAG to collagen ratios in the disc decreased significantly to an average of 0.9 : 1.

Aggrecan mRNA levels were examined following tungsten exposure since it is the main contributor to the sulphated glycosaminoglycan content of the tissue and, hence, is responsible for tissue swelling and function. Furthermore, aggrecan loss is a feature of disc degeneration. Tungsten exposure led to a significant decrease in *Acan* expression in both the AF ($p = 0.0059$) and NP ($p = 0.0008$), when compared with control (Fig. 4**a**).

Collagen mRNA levels were examined following tungsten exposure since collagen fibrils allow the IVD to entrap the proteoglycan aggregates as well as provide tensile strength to the tissue. Although there was a slight increase in *Col1a1* expression in the NP and a decrease in the AF when compared with control (Fig. 4**b**), this was not statistically significant. In contrast, tungsten exposure led to a significant increase in *Col2a1* expression in both the NP ($p = 0.0005$) and AF ($p = 0.0317$), when compared with control (Fig. 4**c**). Immunohistochemistry of IVDs from tungsten-exposed mice corroborated the gene expression results, as demonstrated by decreases in the overall intensity of aggrecan and increased deposition of type II collagen (Fig. 4**d**; black arrows). This was consistent amongst all treated animals.

Since metalloproteinases, particularly members of the ADAMTS and MMP families, are major contributors to aggrecan degradation and loss in disc degeneration, *Mmp1*, *Mmp3*, *Mmp13*, *Adamts4* and *Adamts5* mRNA levels were also examined. Tungsten exposure led to an increase in *Mmp1* expression in both AF and NP tissues, although these changes were not statistically significant (Fig. 5**a**). On the other hand, the increase in *Mmp3* was statistically significant in both the AF ($p = 0.0423$) and NP ($p = 0.0167$), while *Mmp13* despite being increased was not statistically significant when compared to controls (Fig. 5**b**,**c**). Tungsten exposure also resulted in an increase in the expression of *Adamts4* ($p = 0.0002$) and *Adamts5* ($p = 0.0008$) in the AF (Fig. 5**d**,**e**). Immunohistochemistry confirmed an increase in protein levels of ADAMTS4 in the AF of discs from tungsten-exposed mice (Fig. 5**f**). This was consistent amongst all treated animals.

The effect of tungsten exposure on the expression of the neurotrophic factors NGF and BDNF as well as the proinflammatory cytokines IL-1β and TNF-α was examined since these are major contributors to the pathophysiology of discogenic low-back pain. The results demonstrated that *Ngf* expression was significantly increased in NP ($p = 0.0233$) and AF ($p = 0.036$) cells following tungsten exposure (Fig. 6**c**). The neurotrophic factor *Bdbf* was also significantly upregulated in AF cells ($p = 0.0371$). Both proinflammatory cytokines *Il1b* and *Tnfa* were significantly upregulated in both NP and AF cells (Fig. 6**a**,**b**). Immunohistochemical analysis also confirmed increases in protein expression in both NP and AF of tungsten-exposed mice (Fig. 6**e**). This was consistent amongst all treated animals.

A striking feature of degenerative disc disease is the dramatic increase in VEGF levels in the disc. Enhanced expression of VEGF increases the levels of inflammatory cytokines and nerve ingrowth into the damaged discs (Burke *et al.*, 2002; Johnson *et al.*, 2015; Kadow *et al.*, 2015). VEGF was analysed to determine the effect of tungsten exposure on nerve ingrowth. In addition, several animal models of disc degeneration show increased IVD innervation by the identification of CGRP (Johnson *et al.*, 2015; Noorwali *et al.*, 2018). CGRP is a neurotransmitter that acts as a pain modulator and its increased production can cause hyperexcitability and sensitisation (Schou *et al.*, 2017). PGP 9.5 was used to stain neurofibres to

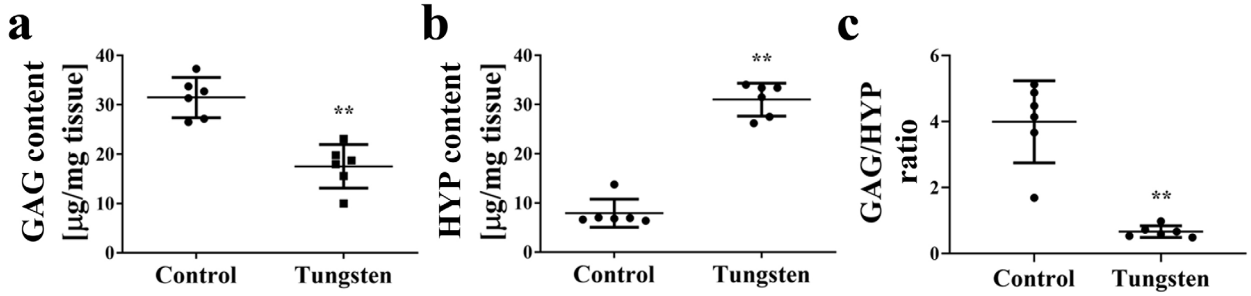

Fig. 3. Tungsten altered the biochemistry of IVD tissue. Lumbar IVDs from individual animals were quantified for (**a**) GAG as a measure of proteoglycan and (**b**) HYP as a measure of collagen content and normalised to wet weight. (**c**) GAG/HYP ratio was used as an indicator of disc fibrosis. Dots represent average result of lumbar discs (L1-5) of individual animals. Lines represent means ± SEMs; Mann-Whitney test, ** $p < 0.01$; $n = 6$ animals.

trace the origin of nerves located at the endplate. Tungsten exposure had no effect on VEGF levels. In contrast, there was a significant upregulation of CGRP ($p = 0.0286$) and PGP9.5 ($p = 0.0290$) in endplate vessels (Fig. 7). In addition, endplate capillaries showed increases in CGRP and PGP9.5 expression as determined on histological sections of mouse IVDs, suggesting the development of sensory neuron invasion of the disc.

Discussion

Upon oral exposure, tungsten markedly accumulated in the vertebrae and IVDs after 4 weeks. This finding was in an agreement with earlier data showing tungsten rapidly deposits in long bones in an insoluble form possibly resembling phosphotungstate (VanderSchee *et al.*, 2018). However, the exact speciation of tungsten in disc tissue remains unknown.

Exposure to tungsten can occur through air, food, water, implanted devices or embedded metal fragments. Air normally contains less than 10 ppt of tungsten. Occupational exposure to higher than background levels of tungsten may occur following use or machining of tungsten metals typically in the form of tungsten carbide. Veterans with embedded fragments or patients with implanted tungsten coils for vascular embolism are at particular risk of exposure since tungsten can leech directly into the circulation. The oral route was chosen because most of the tungsten from any source, when left in the environment or in the body, will oxidize to tungstate (WO_4^{2-}), a thermodynamically stable, mobile, soluble molecule. This issue is pertinent to the wider discussion of whether prolonged oral exposure to tungsten or tungsten compounds can cause disc degeneration in humans or whether it is inert. Although the latter interpretation has been widely favoured, the present results add to the growing urgency calling this assumption into question.

The study foremost findings confirmed that disc cells perceived signals generated following oral exposure to sodium tungstate and responded to them by decreasing disc height and proteoglycan content while increasing collagen synthesis. This also led to a significant decrease in *Acan* expression in both AF and NP. Although tungsten did not affect *Col1a1* expression in NP or AF cells, it did induce a significant increase in *Col2a1* expression. Increased synthesis of collagen type II was also observed in the IVD of tungsten-exposed mice, particularly in the AF. Although tungsten is known to induce fibrosis in lung and liver, in these tissues, deposition of

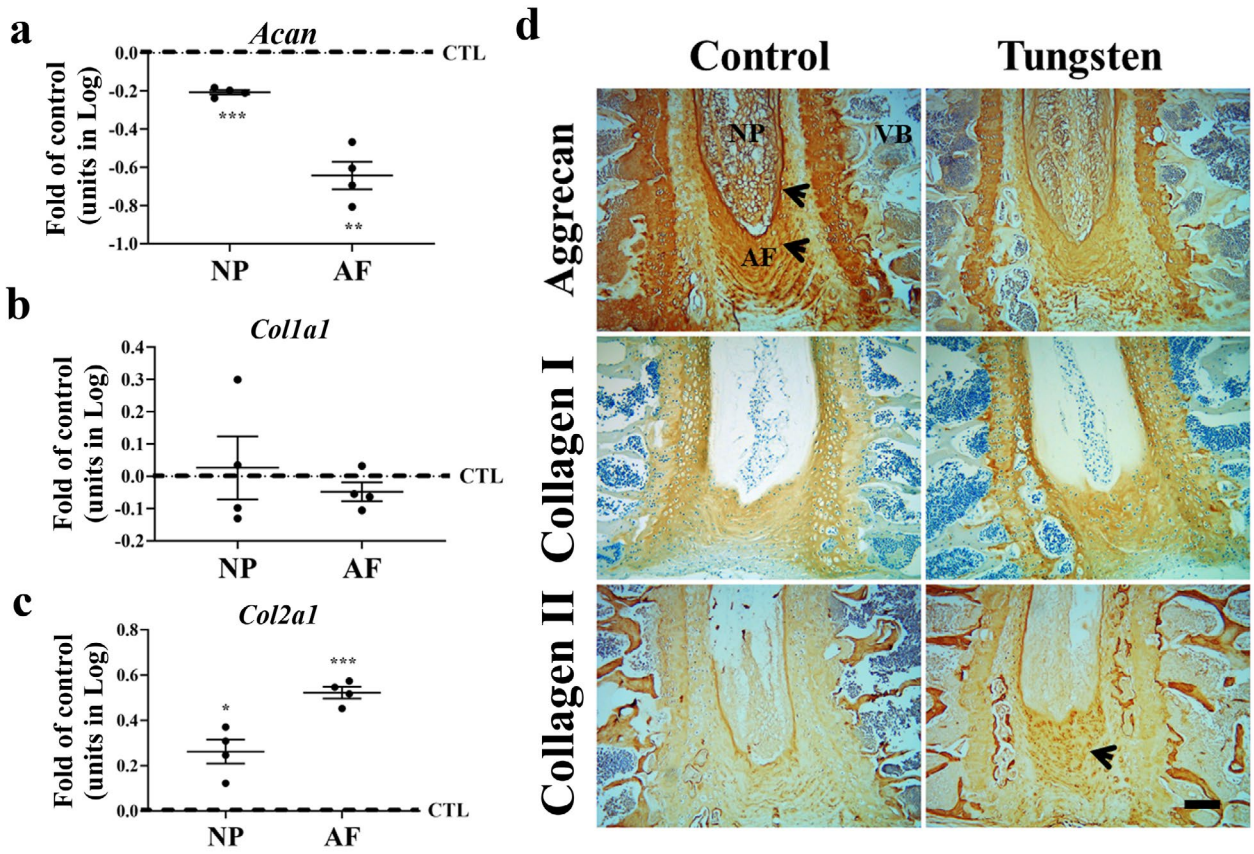

Fig. 4. Effect of tungsten on IVD matrix protein synthesis. Bovine NP and AF cells incubated with 15 ppm tungsten for 6 d and quantified by qPCR for the expression of (**a**) *Acan*, (**b**) *Col1a1* and (**c**) *Col2a1* and compared to controls. Results are presented as Log_{10}. Lines represent means ± SEMs, $n = 4$; two-way ANOVA, *post-hoc* Sidak's multiple comparison's test; * $p < 0.05$; ** $p < 0.01$; *** $p < 0.001$. (**d**) Immunohistochemistry of murine lumbar spines from mice exposed to 15 ppm tungsten for the presence of aggrecan and collage type I and II in IVD tissue. VB: vertebral body. Scale bar: 50 μm.

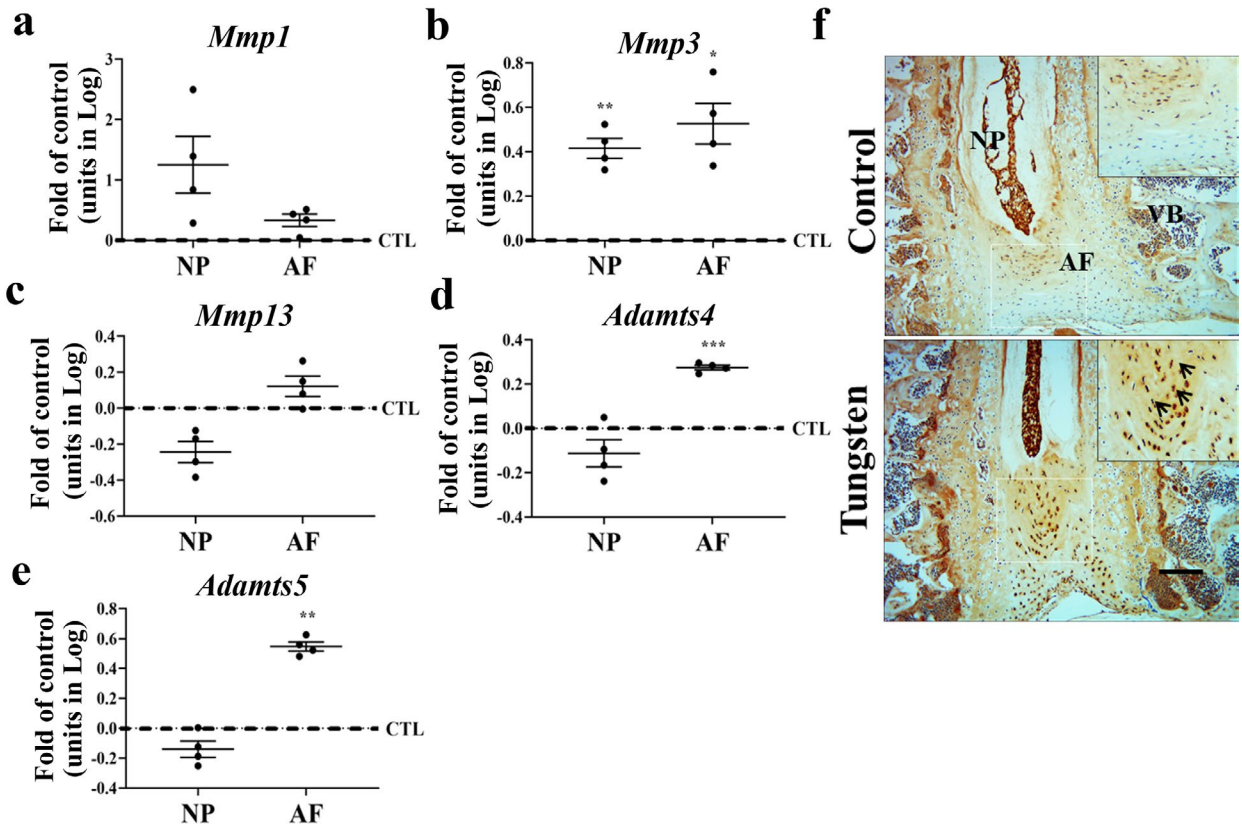

Fig. 5. Altered expression of IVD-associated catabolic enzymes by tungsten exposure. Bovine NP and AF cells incubated with 15 ppm tungsten for 6 d and quantified by qPCR for the expression of (**a**) *Mmp1*, (**b**) *Mmp3*, (**c**) *Mmp13*, (**d**) *Adamts4* and (**e**) *Adamts5* and compared to controls. Results are presented as Log_{10}. Lines represent means ± SEMs, $n = 4$; two-way ANOVA, *post-hoc* Sidak's multiple comparison's test; * $p < 0.05$; ** $p < 0.01$; *** $p < 0.001$. (**f**) Immunohistochemistry of murine lumbar spines from mice exposed to 15 ppm tungsten for the presence of ADAMTS4 in IVD tissue. VB: vertebral body. Scale bar: 50 μm.

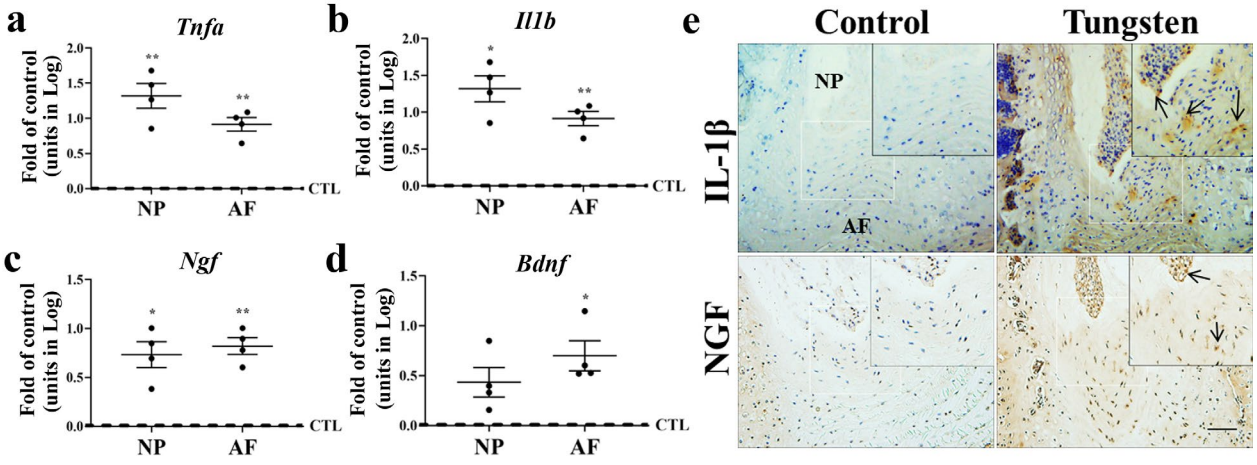

Fig. 6. Tungsten altered the expression of inflammatory and neurotrophic factor in IVD cells. Bovine NP and AF cells incubated with 15 ppm tungsten for 6 d and quantified by qPCR for the expression of (**a**) *Tnfa*, (**b**) *Il1b*, (**c**) *Ngf*, (**d**) *Bdnf* and compared to controls. Results are presented as Log_{10}. Lines represent means ± SEMs, $n = 4$; two-way ANOVA, *post-hoc* Sidak's multiple comparison's test; * $p < 0.05$; ** $p < 0.01$. (**e**) Immunohistochemistry of murine lumbar spines from mice exposed to 15 ppm tungsten for the presence of IL-1β and NGF in IVD tissue. VB: vertebral body. Scale bar: 50 μm.

collagen type I and III are typically observed (Bolt *et al.*, 2016; Knudsen *et al.*, 2017; Tanaka *et al.*, 2014). In an early experimental osteoarthritic model in dogs, collagen type II was found to be upregulated and not downregulated or degraded as is the case in developed or advanced osteoarthritis (Antoniou *et al.*, 1996). Since cartilage and IVD share similar characteristics, it may be possible that upregulation of collagen type II and development of fibrosis are markers of early disc degeneration (Antoniou *et al.*, 1996; Yee *et al.*, 2016). In addition to stimulating collagen gene expression, tungsten also enhanced the expression of catabolic enzymes responsible for extracellular matrix degradation. Tungsten exposure not only decreased the expression of the proteoglycan aggrecan, an important extracellular matrix protein necessary for maintaining disc hydration and compressibility, it also increased enzymes responsible for its degradation.

The next most striking finding was that *Ngf*, *Bdnf*, *Il1b* and *Tnfa* expressions were significantly upregulated in the NP and AF of mice exposed to tungsten. NGF and BDNF are widely known pain mediators (Pezet and McMahon, 2006) and play a critical role in the modulation of low-back pain and osteoarthritis (Brown *et al.*, 2012; Lane *et al.*, 2010; Seidel *et al.*, 2013). The neutralisation of NGF with tanezumab, an anti-NGF monoclonal antibody, has robust analgesic effects on pain (Brown *et al.*, 2012; Lane *et al.*, 2010). Oral exposure of mice to tungsten, clearly generates a potent NGF upregulation and, thus, it is not surprising that its actions are mediated by inflammatory cytokines such as IL-1β and TNF-α (Manni and Aloe, 1998; Manni *et al.*, 2003). Traditionally, inflammation has mostly been identified as being detrimental and correlated with not only disease progression but also back pain (Burke *et al.*, 2002; Johnson *et al.*, 2015). In this

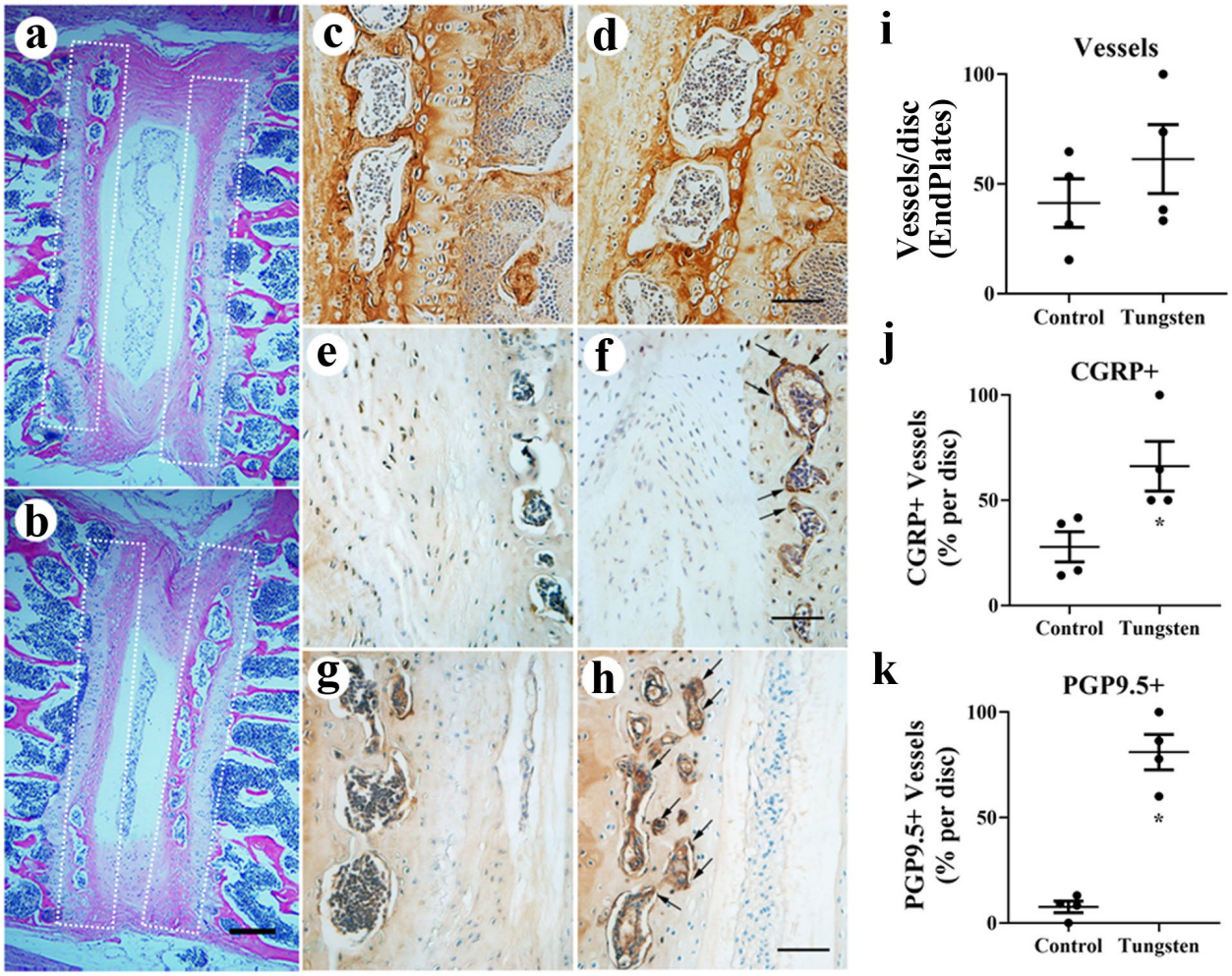

Fig. 7. Tungsten increased the presence of pain-related factors in end-plate capillaries of lumbar discs. Histology and immunohistochemistry on spines from mice fed with (**a**,**c**,**e**,**g**) tap water (control) or (**b**,**d**,**f**,**h**) 15 ppm tungsten-supplemented water for 4 weeks. (**a**,**b**) Representative images of haematoxylin and eosin staining. Immunohistochemistry for (**c**,**d**) VEGF to identify end-plate capillaries, (**e**,**f**) CGRP, a neuronal pain factor, and (**g**,**h**) PGP9.5, a neuronal marker, at end-plate vessels. (**i**) Average number of end-plate vessels per lumbar disc in individual control and tungsten-exposed mice. Average percentage of (**j**) CGRP- and (**k**) PGP9.5-expressing vessels per lumbar disc in individual control and tungsten-exposed mice. Dots represent average value from lumbar discs (L1-5) from individual animals. Lines represent means ± SEMs, $n = 4$ animals; Mann-Whitney test, * $p < 0.05$. VB: vertebral body. Scale bars: (**a**,**b**) 200 μm; (**c**-**h**) 50 μm.

respect, the actions of tungsten are similar to classic agents that stimulate disc degeneration and invoke inflammation.

CGRP and PGP9.5 were also markedly upregulated in vertebral endplates of tungsten-exposed mice. CGRP is a 37-amino-acid neuropeptide that belongs to a family of peptides including adrenomedullin, amylin and calcitonin with diverse biological functions in the periphery and in the central nervous system (Amara *et al.*, 1982). CGRP is widely distributed in nociceptive pathways in human peripheral and central nervous system and its receptors are also expressed in pain pathways. CGRP levels have a positive correlation with pain (Schou *et al.*, 2017). Increased CGRP levels were reported in plasma, synovial and cerebrospinal fluid in subjects with musculoskeletal pain. Similarly, the density of PGP9.5-immunoreactive nerve fibres in patients was positively correlated with the severity of pain (Yao *et al.*, 2010). The increased presence of CGRP and PGP9.5 in vertebral endplates suggested the development of sensory neuron invasion of the disc.

Several questions remain on the localisation of tungsten in the disc. Since the disc is avascular, it is more likely that tungsten would need to diffuse through the endplates of bony vertebrae to accumulate in disc tissue. The endplates consist of a thin cortical layer and hyaline cartilage. Higher concentrations of tungsten were evident in the cortical endplates of vertebrae in the LA-ICP-MS maps of treated mice, suggesting a localised accumulation for diffusion into the disc. Similar findings were observed in the incorporation of tungsten in the long bones of tungsten-exposed mice, where cortical bone was a site of higher concentration (VanderSchee *et al.*, 2018). Bone tissue has been described as the main site of tungsten accumulation; however, in light of these findings, it would indicate that disc tissue is also a primary target. This observation raises the possibility that the vertebrae and IVDs are accumulation organs for tungsten in humans and that the increasing concentrations detected in these tissues could be due to direct deposition to the motion segment. Strikingly, the presence of tungsten was observed in the discs of mice even following 12 weeks of washout, suggesting a slow diffusion similar to that observed in bone (VanderSchee *et al.*, 2018). This may indicate that either tungsten is slow to diffuse, is bound to matricellular proteins such as collagen or both. Notwithstanding, the effects of tungsten on the disc may extend beyond its acute removal following prolonged exposure. Future studies are required to determine the adverse effects of tungsten on disc biology and pain behaviour following chronic exposure.

An additional question surrounds the mechanism(s) of tungsten in altering disc biochemistry. The changes that were observed in 4-week tungsten-exposed mice suggested a pattern of early disc degeneration. There are increasing reports indicating that oxidative stress from ROS and cellular senescence play important roles in the aging and degeneration of IVDs (Hou *et al.*, 2014; Patil *et al.*, 2019). ROS also mitigate disc cell growth and induce DNA damage. Several toxicological reports have demonstrated that tungsten induces the formation of ROS resulting in DNA damage and impairment in DNA repair. Significant increases in apoptotic DNA fragmentation were observed following exposure of tungsten and other metals such as cobalt, commonly used in tungsten alloys (Wasel and Freeman, 2018). Notwithstanding, mice exposed to tungsten exhibit altered B lymphocyte differentiation and increased Gr1+ myeloid-derived suppressor cells, suggesting the potential for increased tumorigenesis (Bolt *et al.*, 2015; Kelly *et al.*, 2013). Further investigation is required to elucidate the role of ROS in tungsten-induced disc degeneration.

The present study was limited to the exposure of 15 ppm tungsten in drinking water. Since the general population is not typically exposed to this level, it is unknown if lower concentrations of tungsten could also bioaccumulate in the disc and whether this could contribute to the development of disc degenerative disease. Since the study used relatively young animals, it is unclear whether the rate or degree of tungsten accumulation in the disc could be affected by age. Bolt *et al.* (2016) showed that age can be a factor in the accumulation of tungsten in bone.

Conclusions

As far as it can be ascertained, the present is the first study describing tungsten deposition in the vertebrae and IVDs *in vivo.* This is also the first study showing that the presence of tungsten in the musculoskeletal system has deleterious biological effects. Collectively, these observations suggested that tungsten affects matrix protein synthesis in IVD cells, enhancing disc fibrosis and increasing the expression of pain markers. Therefore, tungsten toxicity may play a role in disc degeneration disease. Continued studies will allow us to address whether the effect of tungsten on disc cells and perhaps sensory neurons can provide a yet unexplored direct link between IVD joint changes and the generation of pain.

Acknowledgements

This research is supported by the Canadian Institutes of Health Research (KKM, FM and JA, DSB, CVS) and the Canada Research Chairs to DSB. This research used the beamline 5-ID (SRX) of the National Synchrotron Light Source II, a US Department of Energy (DOE) Office of Science User Facility operated for the DOE Office of Science by Brookhaven National Laboratory under Contract No. DE-SC0012704. We thank Brian Jackson Dartmouth for his assistance at the Dartmouth Trace Element Analysis Lab. Trace

Element Analysis Core is supported by NCI Cancer Centre Support Grant 5P30CA023108-37 and NIEHS Superfund grant P42 ES007373.

FM, MPG, KKM and JA conceptualised the experiments and MPG, FM, KKM and LMP supervised the work. HC and AB performed the *in vivo* experiments. MPG performed the *in vitro* experiments and collected the data; CRV and DK performed the LA-ICP-MS and SR-μXRF experiments; MPG performed the statistical analysis. MPG, FM, JA, CRV, LME, KKM and SB prepared the manuscript; MPG and CRV prepared the figures.

The authors have no financial or non-financial conflicts of interest to disclose.

References

Amara SG, Jonas V, Rosenfeld MG, Ong ES, Evans RM (1982) Alternative RNA processing in calcitonin gene expression generates mRNAs encoding different polypeptide products. Nature **298**: 240-244.

Antoniou J, Steffen T, Nelson F, Winterbottom N, Hollander AP, Poole RA, Aebi M, Alini M (1996) The human lumbar intervertebral disc: evidence for changes in the biosynthesis and denaturation of the extracellular matrix with growth, maturation, ageing, and degeneration. J Clin Invest **98**: 996-1003.

Bachthaler M, Lenhart M, Paetzel C, Feuerbach S, Link J, Manke C (2004) Corrosion of tungsten coils after peripheral vascular embolization therapy: influence on outcome and tungsten load. Catheter Cardiovasc Interv **62**: 380-384.

Barbosa I, Garcia S, Barbier-Chassefiere V, Caruelle JP, Martelly I, Papy-Garcia D (2003) Improved and simple micro assay for sulfated glycosaminoglycans quantification in biological extracts and its use in skin and muscle tissue studies. Glycobiology **13**: 647-653.

Barrett J, Wells I, Riordan R, Roobottom C (2000) Endovascular embolization of varicoceles: resorption of tungsten coils in the spermatic vein. Cardiovasc Intervent Radiol **23**: 457-459.

Bolt AM, Grant MP, Wu TH, Flores Molina M, Plourde D, Kelly AD, Negro Silva LF, Lemaire M, Schlezinger JJ, Mwale F, Mann KK (2016) Tungsten promotes sex-specific adipogenesis in the bone by altering differentiation of bone marrow-resident mesenchymal stromal cells. Toxicol Sci **150**: 333-346.

Bolt AM, Mann KK (2016) Tungsten: an emerging toxicant, alone or in combination. Curr Environ Health Rep **3**: 405-415.

Bolt AM, Sabourin V, Molina MF, Police AM, Negro Silva LF, Plourde D, Lemaire M, Ursini-Siegel J, Mann KK (2015) Tungsten targets the tumor microenvironment to enhance breast cancer metastasis. Toxicol Sci **143**: 165-177.

Brown MT, Murphy FT, Radin DM, Davignon I, Smith MD, West CR (2012) Tanezumab reduces osteoarthritic knee pain: results of a randomized, double-blind, placebo-controlled phase III trial. J Pain **13**: 790-798.

Burke JG, Watson RW, McCormack D, Dowling FE, Walsh MG, Fitzpatrick JM (2002) Intervertebral discs which cause low back pain secrete high levels of proinflammatory mediators. J Bone Joint Surg Br **84**: 196-201.

Burleigh MC, Barrett AJ, Lazarus GS (1974) Cathepsin B1. A lysosomal enzyme that degrades native collagen. Biochem J **137**: 387-398.

Domingo JL (2002) Vanadium and tungsten derivatives as antidiabetic agents: a review of their toxic effects. Biol Trace Elem Res **88**: 97-112.

Gaitens JM, Condon M, Squibb KS, Centeno JA, McDiarmid MA (2017) Metal exposure in veterans with embedded fragments from war-related injuries: early findings from surveillance efforts. J Occup Environ Med **59**: 1056-1062.

Grant MP, Epure LM, Bokhari R, Roughley P, Antoniou J, Mwale F (2016) Human cartilaginous endplate degeneration is induced by calcium and the extracellular calcium-sensing receptor in the intervertebral disc. Eur Cell Mater **32**: 137-151.

Guandalini GS, Zhang L, Fornero E, Centeno JA, Mokashi VP, Ortiz PA, Stockelman MD, Osterburg AR, Chapman GG (2011) Tissue distribution of tungsten in mice following oral exposure to sodium tungstate. Chem Res Toxicol **24**: 488-493.

Hou G, Lu H, Chen M, Yao H, Zhao H (2014) Oxidative stress participates in age-related changes in rat lumbar intervertebral discs. Arch Gerontol Geriatr **59**: 665-669.

Hoy D, March L, Brooks P, Blyth F, Woolf A, Bain C, Williams G, Smith E, Vos T, Barendregt J, Murray C, Burstein R, Buchbinder R (2014) The global burden of low back pain: estimates from the Global Burden of Disease 2010 study. Ann Rheum Dis **73**: 968-974.

Johnson ZI, Schoepflin ZR, Choi H, Shapiro IM, Risbud MV (2015) Disc in flames: roles of TNF-α and IL-1β in intervertebral disc degeneration. Eur Cell Mater **30**: 104-116.

Kadow T, Sowa G, Vo N, Kang JD (2015) Molecular basis of intervertebral disc degeneration and herniations: what are the important translational questions? Clin Orthop Relat Res **473**: 1903-1912.

Keith LS, Moffett DB, Rosemond ZA, Wohlers DW (2007a) ATSDR evaluation of health effects of tungsten and relevance to public health. Toxicol Ind Health **23**: 347-387.

Keith LS, Wohlers DW, Moffett DB, Rosemond ZA (2007b) ATSDR evaluation of potential for human exposure to tungsten. Toxicol Ind Health **23**: 309-345.

Kelly AD, Lemaire M, Young YK, Eustache JH, Guilbert C, Molina MF, Mann KK (2013) *In vivo* tungsten exposure alters B-cell development and increases DNA damage in murine bone marrow. Toxicol Sci **131**: 434-446.

Knudsen L, Ruppert C, Ochs M (2017) Tissue remodelling in pulmonary fibrosis. Cell Tissue Res **367**: 607-626.

Lalak NJ, Moussa SA (2002) 'Corrosion' of tungsten spirale coils in the genitourinary tract. Clin Radiol **57**: 305-308.

Lane NE, Schnitzer TJ, Birbara CA, Mokhtarani M, Shelton DL, Smith MD, Brown MT (2010) Tanezumab for the treatment of pain from osteoarthritis of the knee. N Engl J Med **363**: 1521-1531.

Leggett RW (1997) A model of the distribution and retention of tungsten in the human body. Sci Total Environ **206**: 147-165.

Lemus R, Venezia CF (2015) An update to the toxicological profile for water-soluble and sparingly soluble tungsten substances. Crit Rev Toxicol **45**: 388-411.

Manni L, Aloe L (1998) Role of IL-1 beta and TNF-alpha in the regulation of NGF in experimentally induced arthritis in mice. Rheumatol Int **18**: 97-102.

Manni L, Lundeberg T, Fiorito S, Bonini S, Vigneti E, Aloe L (2003) Nerve growth factor release by human synovial fibroblasts prior to and following exposure to tumor necrosis factor-alpha, interleukin-1 beta and cholecystokinin-8: the possible role of NGF in the inflammatory response. Clin Exp Rheumatol **21**: 617-624.

Mort JS, Roughley PJ (2007) Measurement of glycosaminoglycan release from cartilage explants. Methods Mol Med **135**: 201-209.

Mwale F, Roughley P, Antoniou J (2004) Distinction between the extracellular matrix of the nucleus pulposus and hyaline cartilage: a requisite for tissue engineering of intervertebral disc. Eur Cell Mater **8**: 58-63.

Nimni ME (1983) Collagen: structure, function, and metabolism in normal and fibrotic tissues. Semin Arthritis Rheum **13**: 1-86.

Noorwali H, Grant MP, Epure LM, Madiraju P, Sampen HJ, Antoniou J, Mwale F (2018) Link N as a therapeutic agent for discogenic pain. JOR Spine **1**: e1008. DOI: 10.1002/jsp2.1008.

Oegema TR, Jr. (1993) Biochemistry of the intervertebral disc. Clin Sports Med **12**: 419-439.

Patil P, Falabella M, Saeed A, Lee D, Kaufman B, Shiva S, Croix CS, Van Houten B, Niedernhofer LJ, Robbins PD, Lee J, Gwendolyn S, Vo NV (2019) Oxidative stress-induced senescence markedly increases disc cell bioenergetics. Mech Ageing Dev **180**: 97-106.

Pezet S, McMahon SB (2006) Neurotrophins: mediators and modulators of pain. Annu Rev Neurosci **29**: 507-538.

Sampara P, Banala RR, Vemuri SK, Av GR, Gpv S (2018) Understanding the molecular biology of intervertebral disc degeneration and potential gene therapy strategies for regeneration: a review. Gene Ther **25**: 67-82.

Schou WS, Ashina S, Amin FM, Goadsby PJ, Ashina M (2017) Calcitonin gene-related peptide and pain: a systematic review. J Headache Pain **18**: 34. DOI: 10.1186/s10194-017-0741-2.

Seidel MF, Wise BL, Lane NE (2013) Nerve growth factor: an update on the science and therapy. Osteoarthritis Cartilage **21**: 1223-1228.

Shiue I (2015) Relationship of environmental exposures and ankylosing spondylitis and spinal mobility: US NHAENS, 2009-2010. Int J Environ Health Res **25**: 322-329.

Szalóki I, Török SB, Injuk J, Van Grieken RE (2004) X-ray spectrometry. Analytical Chemistry **76**: 3445-3470.

Tanaka J, Moriyama H, Terada M, Takada T, Suzuki E, Narita I, Kawabata Y, Yamaguchi T, Hebisawa A, Sakai F, Arakawa H (2014) An observational study of giant cell interstitial pneumonia and lung fibrosis in hard metal lung disease. BMJ Open **4**: e004407. DOI: 10.1136/bmjopen-2013-004407.

Tajima Y (2001) Lacunary-substituted undecatungstosilicates sensitize methicillin-resistant *Staphylococcus aureus* to beta-lactams. Biol Pharm Bull **24**: 1079-1084.

Tajima Y (2003) Effects of tungstosilicate on strains of methicillin-resistant *Staphylococcus aureus* with unique resistant mechanisms. Microbiol Immunol **47**: 207-212.

VanderSchee CR, Kuter D, Bolt AM, Lo F-C, Feng R, Thieme J, Chen-Wiegart Y-cK, Williams G, Mann KK, Bohle DS (2018) Accumulation of persistent tungsten in bone as *in situ* generated polytungstate. Communications Chemistry **8**. DOI: 10.1038/s42004-017-0007-6.

Vo NV, Hartman RA, Patil PR, Risbud MV, Kletsas D, Iatridis JC, Hoyland JA, Le Maitre CL, Sowa GA, Kang JD (2016) Molecular mechanisms of biological aging in intervertebral discs. J Orthop Res **34**: 1289-1306.

Wasel O, Freeman JL (2018) Comparative assessment of tungsten toxicity in the absence or presence of other metals. Toxics **6**: 66. DOI: 10.3390/toxics6040066.

Watanabe H, Yamada Y, Kimata K (1998) Roles of aggrecan, a large chondroitin sulfate proteoglycan, in cartilage structure and function. J Biochem **124**: 687-693.

Yao HJ, Huang XF, Lu BC, Zhou CY, Zhang J, Zhang XM (2010) [Protein gene product 9.5-immunoactive nerve fibers and its clinical significance in endometriotic peritoneal lesions]. Zhonghua Fu Chan Ke Za Zhi **45**: 256-259.

Yee A, Lam MP, Tam V, Chan WC, Chu IK, Cheah KS, Cheung KM, Chan D (2016) Fibrotic-like changes in degenerate human intervertebral discs revealed by quantitative proteomic analysis. Osteoarthritis Cartilage **24**: 503-513.

Zoroddu MA, Medici S, Peana M, Nurchi VM, Lachowicz JI, Laulicht-Glickc F, Costa M (2018) Tungsten or wolfram: friend or foe? Curr Med Chem **25**: 65-74.

Web References

1. https://github.com/davidkuter/ICP-MS [12-04-2021]

2. https://github.com/NSLS-II-HXN/PyXRF [12-04-2021]

Discussion with Reviewers

Svenja Illien-Junger: Metabolic studies in mice have demonstrated sex-dependent differences in response to diet (Ingvorsen *et al.*, 2017, additional reference). In the present study only male mice were used to study the effect of orally administered tungsten. Could you please speculate about the possibility of sex-dependent differences?
Authors: This is a very interesting point. In a previous report investigating the effects of tungsten in mice, sex-dependent differences in adipogenesis in bone were observed (Bolt *et al.*, 2016.) However, in preliminary data, no similar trends on the effects of tungsten on disc height and GAG content were observed. Further studies are required to determine any sex-dependent differences on disc degenation and markers of inflammation and pain.

Svenja Illien-Junger: Why did you not distinguish between sex? Especially measurements of disc height and vertebral changes might be sex dependent.
Authors: This is an interesting question but due to limited animal numbers we have decided to remove the females from the study.

Graciosa Teixeira: Why did the authors choose the administration protocol of 15 ppm for 4 weeks in mice? Is this clinically relevant? Does this protocol simulate a similar exposure as it may happen in humans?
Authors: The purpose of using the concentration of 15 ppm tungsten was to determine if the upper limit set by certain regions is non-toxic. There are very few countries that monitor tungsten in their potable water. For instance, Russia has set the limit at 5 ppm, whereas the Commonwealth of Massachusetts has set it to 15 ppm. A period of 4 weeks was based on a previous study on the effect of tungsten on bone (Bolt *et al.*, 2016); however, future work will need to be performed to establish a minimum exposure limit for disc.

Graciosa Teixeira: After tungsten exposure, the most is released with urine. Which is the percentage that is retained in the body? For how long is it expected to stay in the human IVD?
Authors: Although most of the tungsten ingested will be excreted through the kidney and gut, approximately 5 % is retained in the body. However, this is dependent on time after and duration of exposure. It is unclear how long tungsten remains in the disc; however, results from the present study indicate that tungsten signatures were still present even following a 12-week washout.

Graciosa Teixeira: Does the developmental stage affect how tungsten is processed in the body? Is there an age range for higher risk of disc herniation, for instance?
Authors: This is an interesting point. Unlike a previous study (Bolt *et al.*, 2016) on bone where developmental stage influenced tungsten accumulation, preliminary evidence indicates that tungsten can freely diffuse into the disc.

Graciosa Teixeira: Although for less time (48 h), cell pellets were treated with the same concentration (15 ppm) of tungsten as animals. AF and NP cells were in direct contact with a lot more tungsten than what arose to the discs *in vivo*. Why not opting for similar concentrations to the ones reaching the discs in the *in vivo* experiments? Physiologically, this would be a more relevant experiment.
Authors: The rationale for the tungsten concentration used was to determine the effects of the upper limit set by certain regions. Certainly, other concentrations need to be tested, including the ~ 3 ppm that bioaccumulated in the discs from tungsten-exposed mice.

Graciosa Teixeira: Could CGRP and PGP9.5 be used as biomarkers for disc herniation?
Authors: Yes, they could since they are markers for the presence of neurons. NGF is expressed in herniated discs (Kadow *et al.*, 2015), therefore it would be important to determine whether this is indicative of nerve infiltration.

Additional Reference

Ingvorsen C, Karp NA, Lelliott CJ (2017) The role of sex and body weight on the metabolic effects of high-fat diet in C57BL/6N mice. Nutr Diabetes **7**: e261. DOI: 10.1038/nutd.2017.6.

Editor's note: The Scientific Editor responsible for this paper was Sibylle Grad.